Fragmentation dynamics of ionized neon clusters (Ne[sub n],n=3–14) embedded in helium nanodroplets

David Bonhommeau, Nadine Halberstadt, Alexandra Viel

Fragmentation dynamics of ionized neon clusters (Ne_n, $n=3–14$) embedded in helium nanodroplets

David Bonhommeau and Nadine Halberstadt[a)]
Laboratoire de Physique Quantique, IRSAMC, UMR 5626, CNRS et Université Paul Sabatier, F-31062 Toulouse Cedex 09, France

Alexandra Viel
PALMS-SIMPA, UMR 6627 du CNRS, Université de Rennes 1, Campus de Beaulieu, F-35042 Rennes, France

(Received 25 July 2005; accepted 28 November 2005; published online 13 January 2006)

We report a theoretical study of the nonadiabatic fragmentation dynamics of ionized neon clusters embedded in helium nanodroplets for cluster sizes up to $n=14$ atoms. The dynamics of the neon atoms is modeled using the molecular dynamics with quantum transitions method of Tully [J. Chem. Phys. **93**, 1061 (1990)] with the nuclei treated classically and transitions between electronic states quantum mechanically. The potential-energy surfaces are derived from a diatomics-in-molecules model to which induced dipole-induced dipole interactions are added. The effect of the spin-orbit interaction is also discussed. The helium environment is modeled by a friction force acting on charged atoms whose speed exceeds the critical Landau velocity. The dependence of the fragment size distribution on the friction strength and on the initial nanodroplet size is investigated. By comparing with the available experimental data obtained for Ne_3^+ and Ne_4^+, a reasonable value for the friction coefficient, the only parameter of the model, is deduced. This value is then used to predict the effect of the helium environment on the dissociation dynamics of larger neon clusters, $n=5–14$. The results show stabilization of larger fragments than in the gas phase, but fragmentation is not completely caged. In addition, two types of dynamics are characterized for Ne_4^+: fast and explosive, therefore leaving no time for friction to cool down the process when dynamics starts on one of the highest electronic states, and slower, therefore leading to some stabilization by helium when it starts on one of the lowest electronic states. © *2006 American Institute of Physics*. [DOI: 10.1063/1.2158993]

I. INTRODUCTION

Because of the absence of a triple point in the phase diagram of bulk helium, helium clusters are the only clusters that are definitely liquid. Superfluid behavior has been theoretically predicted for clusters as small as 64 atoms[1] and experimentally observed shortly after.[2] Since then, one major goal in the current research on helium clusters has been to search for experimental manifestation of superfluid behavior at the microscopic level. Many of the well-known superfluid phenomena such as singularity in the heat capacity or superfluid flow which have been evidenced in bulk helium are not accessible in the finite-size helium clusters. To date the only well-documented microscopic manifestation of superfluidity, the so-called microscopic Andronikashvili experiment,[2] has been proven by investigating the rotation spectra of molecules embedded in helium clusters, and many experimental as well as theoretical investigations have been dedicated to this subject.[3–11] Spectroscopic studies of atoms and molecules embedded in large helium droplets have been performed in order to characterize collective excitations of the helium atoms,[12–15] but recent experiments seem to show that the spectra are dominated by the structure of the nonsuperfluid solvation layer around the guest molecule.[16–18]

Another way to study microscopic manifestations of superfluidity is to compare the dissociation dynamics of molecular systems in the gas phase and inside helium clusters. Two opposite behaviors can be expected. Because of the high heat capacity of superfluid helium, there can be very rapid quenching of the gas phase fragmentation process and fragmentation can be hindered or even completely quenched. On the other hand, particles moving inside superfluid helium at a velocity below the critical Landau velocity are expected to move without friction, which should leave the fragmentation process unaltered. The first attempt to study the effects of helium clusters on molecular ion fragmentation was performed on SF_6 by Toennies and co-workers.[19,20] The fragmentation of SF_6^+ to SF_5^+ was too fast to be affected, but further fragmentation was completely suppressed indicating very efficient cooling. In a similar experiment, Callicoatt *et al.*[21] observed that in droplets containing more than 15 000 atoms, only 10% of the $(NO)_2^+$ ions fragmented to $NO^+ + NO$. Experiments performed on ionized rare-gas clusters by Janda and co-workers[22–24] have shown that these rare-gas clusters fragment to a lesser extent when they are ionized inside helium clusters, compared to their fragmentation in the gas phase. In a recent experiment, Lewis *et al.*[25] have demonstrated that the triphenylmethanol hot molecular ion was efficiently cooled by the helium droplets. In addition,

[a)]Electronic mail: nadine.halberstadt@irsamc.ups-tlse.fr

their results suggest that the first 5000 helium atoms remove roughly 22 cm^{-1}/at. from the molecular ion, which is much more than the 5 cm^{-1}/at. expected from thermal evaporation. On the other hand, the cooling from 10 000 to 40 000 atoms corresponds to only 0.16 cm^{-1}/at., much less than the thermal value. The fact that the cooling by helium clusters is also efficient for neutral species was shown by Braun and Drabbels[26] in a recent experiment on the photodissociation of CH_3I. Their results were surprisingly well reproduced by a hard-sphere collision model. From a theoretical point of view, the only work published to date on the cooling exerted by helium is a study by Takayanagi and Shiga[27] on the photodissociation dynamics of Cl_2 embedded in helium droplets. They predicted that cage effects reduce the relative translational energy of the Cl atoms, and that these effects largely decrease when the helium motion is treated quantum mechanically by a path-integral centroid molecular-dynamics approach.

Rare-gas clusters constitute ideal model systems to study the influence of the helium environment on a dissociative event. They are known for fragmenting extensively upon ionization in the gas phase,[28–31] due to the large difference between the neutral van der Waals bonding and the much stronger ionic bonding. Vertical ionization produces the cluster ions in a configuration containing a large amount of internal energy, which induces extensive dissociation. Experiments by Janda and co-workers on argon,[22] neon,[23] and xenon[24] clusters have shown that their fragmentation is significantly hindered, and can even be caged, in helium nanodroplets.

In a recent publication,[32] we have studied the fragmentation of free neon clusters upon ionization for clusters with 3–14 atoms, taking into account all the potential-energy surfaces involved and their couplings. Fragmentation was found to be quite extensive: Ne_2^+ was the main fragment for all sizes, with a maximum proportion of 99% for Ne_9. Ne^+ was the second main fragment for smaller sizes and Ne_3^+ for larger sizes. Analysis of the fragmentation showed that the mechanism was rather explosive, with several atoms dissociating at the same time.

The purpose of this work is to determine the role of the helium environment in the dissociation of ionized neon clusters. Is there no effect since these nanodroplets are known to be superfluid, or is any dissociation inhibited because of the very high heat conductivity of superfluid helium? The interest of this question is not only fundamental, it is practical as well. One of the most common experimental tools to study host molecules or clusters inside helium nanodroplets is mass spectrometry, which implies an ionization step. This ionization usually produces fragmentation of the host molecule or cluster, and it is important to understand the fragmentation process in order to be able to reproduce the inital neutral size distribution.

In this study the ionized neon clusters are treated using the same method as in our previous work on isolated neon clusters,[32] and the helium environment is described in a phenomenological way as in our earlier study on the dissociative ionization of Ne_3 inside helium droplets.[33] In order to cover the whole range of possible behaviors, we introduce a friction force acting on the neon atoms proportionally to their instantaneous charge as long as their velocity is larger than the Landau critical velocity. Given the low temperature (0.4 K), the Langevin random force describing how energy is transferred from the helium bath to the neon cluster is neglected. The friction coefficient is the only adjustable parameter in our model. A small value of the friction coefficient would reveal a weak interaction between the helium droplet and the dissociating system, while a large value would indicate a strong hindering of the dissociation dynamics due to high heat conductivity. Ion drift experiments have been conducted in liquid, superfluid helium to characterize the friction exerted by bulk helium on a moving charged atom. For Na^+ the resulting ion mobility corresponds to a friction coefficient of 0.078 a.u.[34] Unfortunately no such experiment has been conducted for Ne^+. The only studies on Ne^+ mobilities have been performed in gaseous helium with pressures that hardly reach 50 μbars,[35,36] so that our study is the first approach to characterize the influence of superfluid helium on the motion of Ne^+.

II. METHOD

A. Description of free Ne_n^+ clusters

The method for describing the dissociation dynamics of free ionized neon clusters has already been described in our earlier publications.[32,33] We briefly recall here the essential features. The potential-energy surfaces and their nonadiabatic couplings are derived from a diatomics-in-molecules (DIM) model to which induced dipole-induced dipole and spin-orbit interactions are added. The ionized neon cluster dynamics is described using the molecular dynamics with quantum transitions (MDQT) method of Tully.[37] The classical nuclei evolve on one adiabatic surface at a time and transitions between electronic states are taken into account by allowing for hops between surfaces. As discussed in our recent work,[32] the nature of the vector along which momenta are adjusted in order to conserve total energy and nuclear angular momentum at a hopping event has very little influence on the results. In the present study, the gradient $\nabla(V_k - V_l)$ of the energy difference between the two potential-energy surfaces involved in the hop has been used. Classically forbidden hops are discarded as advocated by Müller and Stock.[38] Initial conditions reproduce in a classical way a vertical ionization from a neutral cluster in its ground vibrational state.

B. Phenomenological modelization of the surrounding helium environment

The helium nanodroplets are assumed to be spherical. Due to the fact that the neon-helium interaction ($D_e \approx 14.7$ cm^{-1}) is stronger than the helium-helium interaction ($D_e \approx 7.6$ cm^{-1}), it is physically reasonable to assume that the neutral neon cluster is initially located close to the center of the droplet. The effect of the helium environment on the ionized neon cluster dynamics is described in a phenomenological way by a friction force acting on the neon atoms inside the droplet when their speeds exceed the Landau critical velocity ($v_{\text{Landau}} = 58$ m/s),[39] as described in our earlier

TABLE I. ^{4}He density ρ_{He} and mean binding energy $E/\langle N\rangle$ obtained close to the center of finite-size nanodroplets of pure ^{4}He using the DFT algorithm developed by Barranco and co-workers (Refs. 41–43), compared to bulk properties (Refs. 44–46).

$\langle N\rangle$	$\rho_{He}(\text{Å}^{-3})$	$E/\langle N\rangle$(K)
1100	0.022 62	5.4
2200	0.022 51	5.8
2800	0.022 47	5.9
3300	0.022 44	6.0
Bulk	0.021 85	7.2

work on the fragmentation dynamics of the neon trimer.[33] Reciprocally, the friction force is assumed to induce an energy transfer from the neon subcluster to the helium nanodroplet. This effect is taken into account in the following way. The kinetic energy lost by the neon atoms because of friction is assumed to be dissipated very rapidly into the helium droplet, leading to the evaporation of helium atoms.[40] This effect was not taken into account in Ref. 33 which considered infinite-size helium droplets. At each step of the dynamics, the number of evaporated atoms is estimated as the ratio of the kinetic-energy loss to the mean binding energy of the pure helium cluster. The resulting diameter of the helium nanodroplet is then deduced from its helium density. Both the mean binding energy and the helium density are determined from a density-functional theory (DFT) algorithm developed by Barranco and co-workers[41–43] for a pure ^{4}He droplet. For simplicity, they are kept constant during the whole propagation time for a given initial nanodroplet size. Their values are collected in Table I for the average nanodroplet sizes reported in the experimental work of Ruchti *et al.*,[23] $\langle N\rangle$=1100, 2200, 2800, and 3300, together with the corresponding bulk values.

III. RESULTS FOR Ne_3 AND Ne_4: COMPARISON WITH EXPERIMENT

A. Branching ratios

The most detailed experimental results by Ruchti *et al.*[23] have been obtained for the branching ratios of the fragments originating from the ionization of Ne_3 and Ne_4. Figure 1 compares the final fragment branching ratios from our simulation to the experimental results for $(Ne_3^+)^*$ and $(Ne_4^+)^*$ parent ions fragmenting inside nanodroplets composed of 1100, 2200, 2800, and 3300 helium atoms. Several values for the friction coefficient are tested: 0.75, 2.5, and 7.5 a.u. Note that both pure Ne_2^+ and Ne_2^+ fragments with helium atoms still attached to the ionic dimer, denoted as $Ne_2He_k^+$, are detected in the experiment. Since it is not possible within our phenomenological approach to distinguish between Ne_2^+ and $Ne_2He_k^+$, we only consider the sum of these species. In the case of the $(Ne_4^+)^*$ parent ion, Ruchti *et al.*[23] only report $P(Ne_3^+)/P(Ne_2^+)$ branching ratios. We have thus adapted these ratios by assuming the same $P(Ne_2^+)/P(Ne_2He_k^+)$ proportion as in the case of the $(Ne_3^+)^*$ parent ion. This rather crude estimate is intended to determine a value of the friction coefficient that is roughly consistent with the data, in order to explore the resulting dynamics of higher clusters. The original and the adapted experimental results are reported in Table II and shown in Fig. 1(b). Since no $Ne_3He_k^+$ fragments are reported, they are assumed to be negligible. This can be due to the larger number of degrees of freedom in Ne_3^+ which favors the "shaking off" of helium atoms during the vibrational relaxation of the Ne_3^+ fragment.

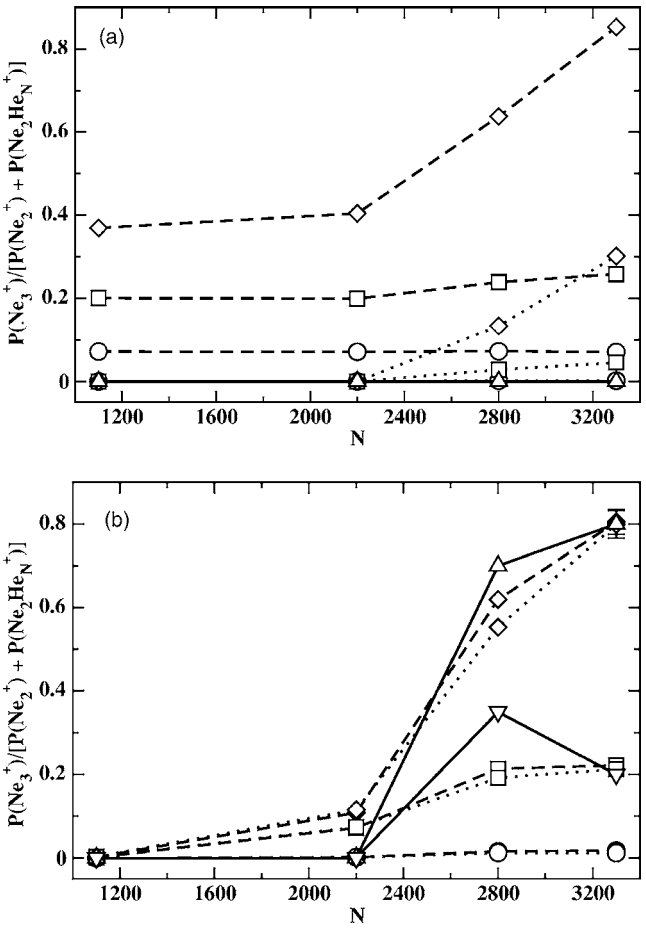

FIG. 1. $P(Ne_3^+)/P(Ne_2^+ + Ne_2He_k^+)$ branching ratios from (a) Ne_3 and (b) Ne_4 ionizations obtained with different values of the friction coefficient (0.75, 2.5, and 7.5 a.u.). The straight lines correspond to the experimental results, and the dashed and dotted lines to the calculations neglecting or including the spin-orbit interaction, respectively. The upward triangles correspond to the original experimental results (Ref. 23) and the downward triangles to the experimental values adapted to take into account Ne_2^+ fragments with helium atoms attached to them (see text). The other symbols correspond to the simulation results with γ=0.75 a.u. (circles), γ=2.5 a.u. (squares), and γ =7.5 a.u. (diamonds). Note that in (a), both the original and the adapted experimental results as well as the γ=0.75 a.u. calculations including spin-orbit coupling are zero for all $\langle N\rangle$ values. The simulated results correspond to averages over 5000 trajectories for each γ value. The corresponding error bars are specified when their amplitude exceeds the size of the plotting symbols.

We also examine the effect of the spin-orbit interaction. In Ref. 33 we have shown that the spin-orbit interaction mainly affects the $(Ne_3^+)^*$ dissociation results, because it separates the electronic states in two groups connecting to the $Ne^+(^2P_{3/2})+2Ne$ and $Ne^+(^2P_{1/2})+2Ne$ asymptotic states in the region accessed by vertical ionization, resulting in a doubly peaked initial energy distribution for the parent ion. In addition, the spin-orbit interaction couples the A' and A'' states which are otherwise uncoupled because of symmetry.

TABLE II. Selected experimental branching ratios from Ne_3 and Ne_4 ionizations for different mean helium droplet sizes $\langle N \rangle$. The first two rows are the experimental results from Ruchti *et al.* (Ref. 23). The $P(Ne_3^+)/P(Ne_2^+ + Ne_2He_k^+)$ branching ratio of the third row is estimated from the data of the first two rows (see text).

$\langle N \rangle$		1100	2200	2800	3300
Ne_3	$P(Ne_2He_4^+)/P(Ne_2^+)$	0	0.2	1	3
Ne_4	$P(Ne_3^+)/P(Ne_2^+)$	…	…	0.7	0.8
	$P(Ne_3^+)/P(Ne_2^+ + Ne_2He_k^+)$	…	…	0.35	0.20

These effects rapidly disappear as the cluster size, hence the number of states, increases and the center of the total-energy distribution shifts to lower energies.

According to the experimental results of Ruchti *et al.*, the ionization of Ne_3 clusters does not lead to any stable Ne_3^+ fragments within experimental uncertainties [$P(Ne_3^+) \leqslant 5\%$ (Ref. 47)]. Our results including spin-orbit interaction agree quite well with this result for the smaller values of the friction coefficients, $\gamma = 0.75$ or 2.5 a.u. As can be seen in Fig. 1(a), the highest friction coefficient tested, $\gamma = 7.5$ a.u., gives a $P(Ne_3^+)/P(Ne_2^+ + Ne_2He_k^+)$ ratio of about 0.3 for the largest nanodroplet size, which clearly overestimates the effect of the friction.

For the fragmentation of $(Ne_4^+)^*$ presented in Fig. 1(b), the experimental results indicate a strong dependence of the proportion of Ne_3^+ fragments as a function of the nanodroplet size. No Ne_3^+ is produced for the smaller sizes, $N = 1100$ or 2200, then the proportion sharply increases for $N = 2800$.[48] This sharp increase is attenuated when $Ne_2He_k^+$ fragments are taken into account. The smallest value of the friction coefficient, $\gamma = 0.75$ a.u., gives a negligible amount of Ne_3^+ fragments for all the helium droplet sizes. The $\gamma = 2.5$ a.u. value reproduces well the adapted experimental results, while $\gamma = 7.5$ a.u. gives ratios close to the original ones (which do not take into account the $Ne_2He_k^+$ fragments) and is therefore clearly overestimated. Based on this analysis, the value of $\gamma = 2.5$ a.u. is used in the remaining of this work since it appears to represent the best compromise when comparing with the experimental data.

The nanodroplet size dependence of the $P(Ne_3^+)/P(Ne_2^+ + Ne_2He_k^+)$ branching ratio can be partly understood in terms of energy dissipation. In our previous work,[32] we have shown that the mean energy released during the dynamics of free $(Ne_4^+)^*$ is 0.66 eV. This value can be compared to the energy needed to completely evaporate helium nanodroplets: 0.52, 1.10, 1.42, and 1.70 eV for $N = 1100$, 2200, 2800, and 3300, respectively. The energy provided by the neon cluster dissociation is thus sufficient to completely evaporate all the helium atoms for the smallest nanodroplet size ($N = 1100$ atoms), but not for the larger ones. This explains the weak $P(Ne_3^+)/P(Ne_2^+ + Ne_2He_k^+)$ branching ratio obtained in Fig. 1(b) for the smallest nanodroplets. Evaporation is not complete in general for larger nanodroplets ($N \geqslant 2200$ atoms) and the proportion of stable Ne_3^+ increases with nanodroplet size until reaching the infinite nanodroplet value for $N = 2800$–3300.

B. Time evolution of the nanodroplet size

In order to get a better understanding of the branching-ratio dependence on the nanodroplet size, the time evolution of the nanodroplet size distribution for each value of the initial average experimental size is presented in Fig. 2. In this figure, the embedded cluster is Ne_4 and the friction coefficient modeling the helium environment is $\gamma = 2.5$ a.u. Spin-orbit interaction is not included since we have shown earlier that it does not affect notably the results for this cluster size. The time evolution of the nanodroplet size distribution revealed by Fig. 2 is very surprising in that it presents a splitting of the original delta-functionlike peak into two peaks. In addition to the expected broadening peak that gradually evolves towards smaller sizes because of evaporating atoms, there is a second peak remaining close to the initial nanodroplet size.

In order to understand the origin of this second peak, we have investigated the effect of the initial electronic state on which the neon atom dynamics starts. Figure 3 presents the mean total energy transferred to the helium environment during the dissociation dynamics of $(Ne_4^+)^*$ as a function of the initial electronic state. The $N = 2200$, 2800, and 3300 curves all fall together, whereas the curve corresponding to the 1100 atom helium droplet clearly shows a much smaller energy tranfer: this is due to the fact that the smallest helium droplets do not contain enough atoms to absorb all the energy. For all the other sizes there is a strong dependence of the total-energy loss on the state on which the dynamics has started. The lowest-energy states (states 1 and 2) release the most energy, states 3–10 release about the same amount of energy, and the highest-energy levels (states 11 and 12) release much less energy than all the other levels. This explains the double peak of nanodroplet size distributions in Fig. 2: the peak remaining near the original nanodroplet size corresponds to trajectories starting on the highest-energy level, since the small energy release allows for the evaporation of only a small number of atoms. The peak moving towards small sizes corresponds to trajectories starting on the lowest-energy levels, for which the large energy release results in the evaporation of a large number of atoms. The trajectories starting on an intermediate state contribute to the broadening of the two extreme peaks.

This is confirmed by Fig. 4, which shows separately the time evolution of the helium droplet size distribution during the $(Ne_4^+)^*$ parent ion dissociation for dynamics starting on the lowest and highest initial energy states, for a nanodroplet size of 3300 atoms. Intermediate energy states combine the behavior of the two extreme states.

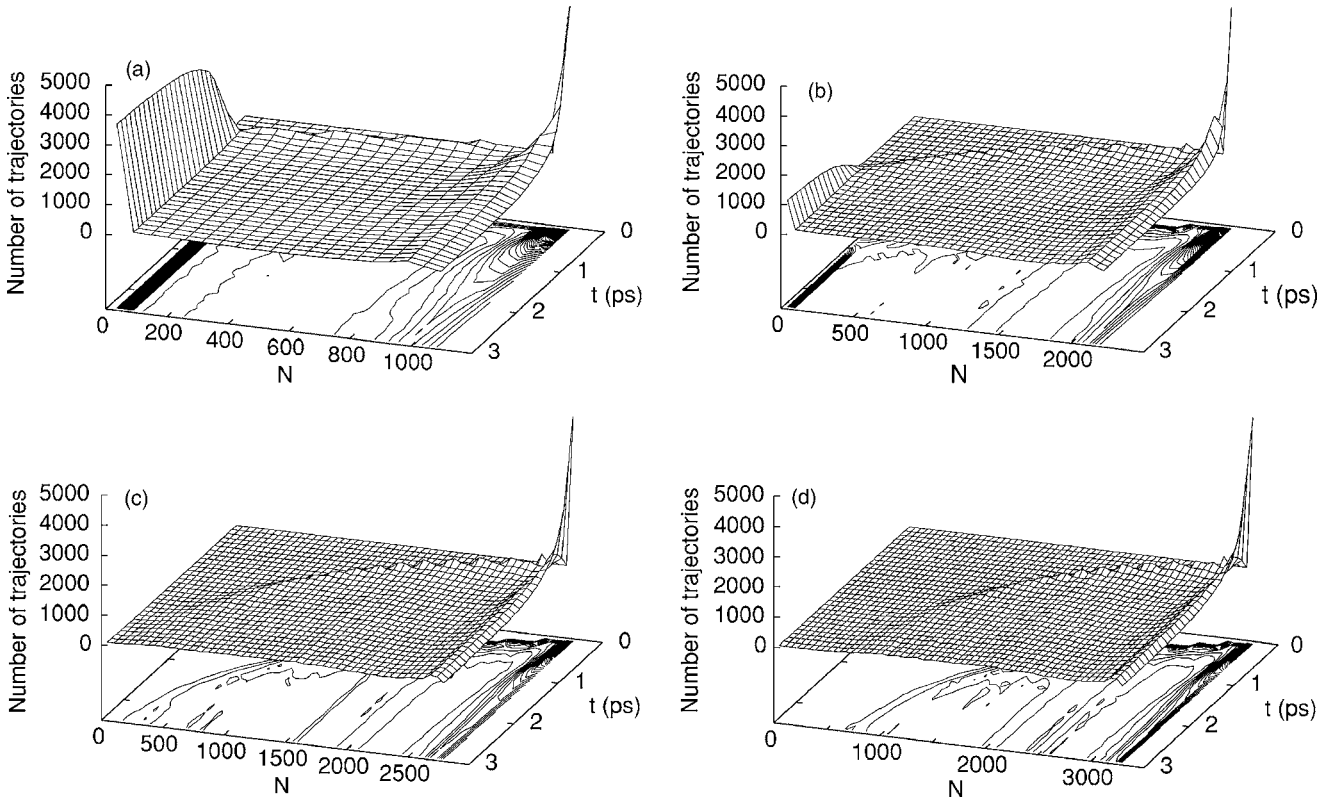

FIG. 2. Time evolution of the nanodroplet size distribution following the ionization of embedded Ne_4. The friction coefficient modeling the helium environment is $\gamma=2.5$ a.u. Plots (a)–(d) correspond to different values of the initial helium nanodroplet size: (a) $N=1100$, (b) $N=2200$, (c) $N=2800$, and (d) $N=3300$. Each of these sizes corresponds to an average experimental size from Ref. 23. Contours on the base plane are spaced by 50 trajectories. These size distributions have been obtained by averaging over 5000 trajectories.

C. Dependence of the final fragment proportions on the initial electronic state

The final fragment proportions also depend on the initial electronic state of the parent ions, as demonstrated in Fig. 5. This figure presents final proportions of fragments for Ne_4 ionization inside a droplet initially composed of 3300 helium atoms, as a function of the initial electronic state. When dy-

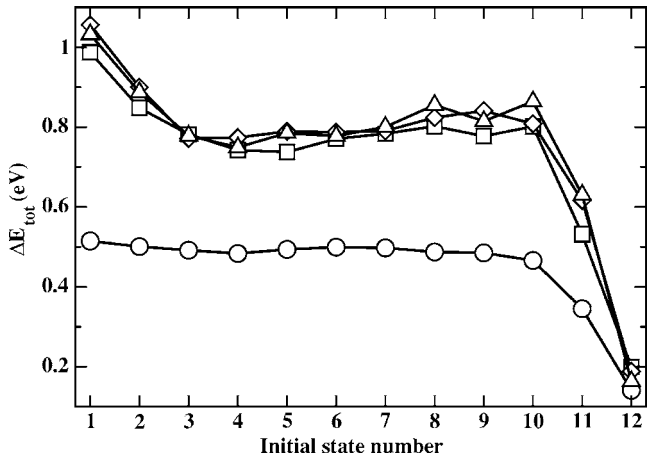

FIG. 3. Mean total energy lost during the dissociation dynamics of $(Ne_4^+)^*$ as a function of the initial electronic state number. The different curves correspond to nanodroplets with $N=1100$ (circles), 2200 (squares), 2800 (diamonds), and 3300 (upward triangles) helium atoms. The friction coefficient modeling the helium environment is $\gamma=2.5$ a.u. The results correspond to an average over 5000 trajectories for each nanodroplet size, so that each point is averaged over around 400 trajectories.

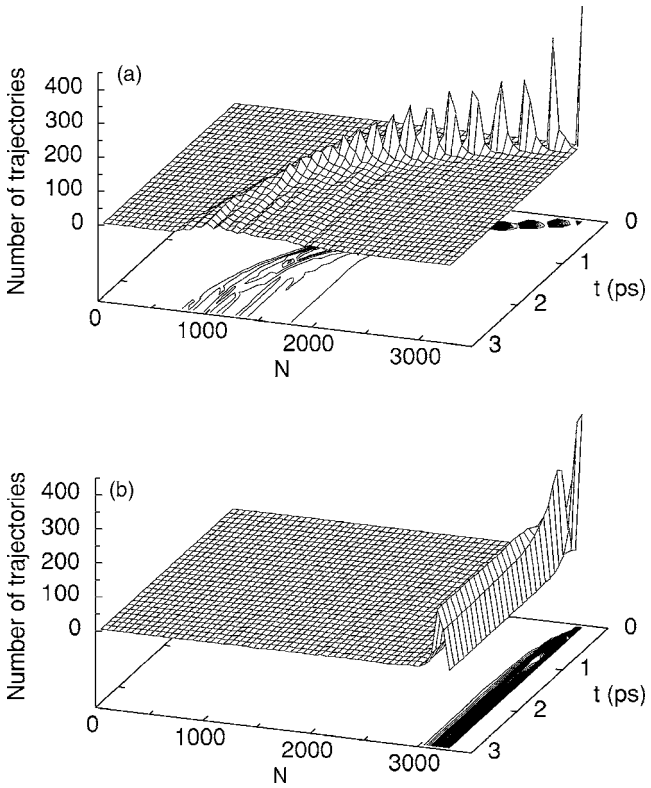

FIG. 4. Time evolution of the nanodroplet size distribution during the dissociation dynamics of the $(Ne_4^+)^*$ parent ion embedded in a nanodroplet initially composed of 3300 helium atoms. Plot (a) corresponds to trajectories for which dynamics begins on the lowest-energy electronic state and plot (b) to trajectories for which dynamics begins on the highest-energy electronic state. Contours on the base plane are spaced by 10 trajectories.

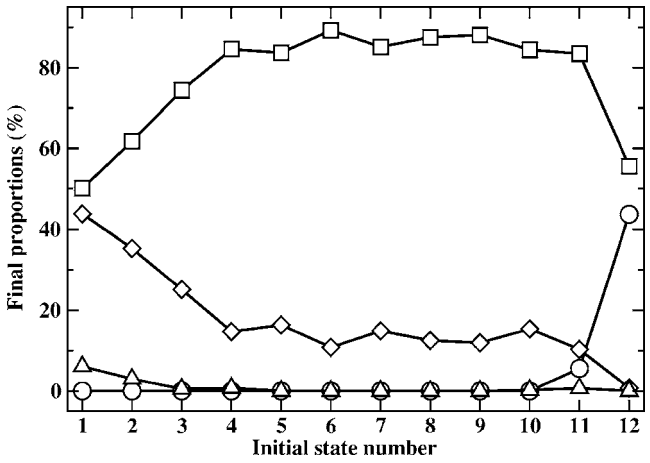

FIG. 5. Final fragment proportions from the ionization of Ne_4 embedded in a 3300-atom nanodroplet, as a function of the initial electronic state: Ne^+ (circles), Ne_2^+ (squares), Ne_3^+ (diamonds), and Ne_4^+ (upward triangles). The friction coefficient modeling the helium environment is $\gamma=2.5$ a.u. The calculation is performed over a set of 5000 trajectories, i.e., about 400 trajectories for each electronic state.

namics starts on one of the three lowest states, the mean size of the fragments is maximum: the proportion of Ne_3^+ and even Ne_4^+ is largest for state 1 and decreases from there. This is due to the larger effect of friction for these states which leads to a larger energy loss, as seen above in Fig. 3. When dynamics starts on one of the states numbered 3–10, the final fragment proportions are nearly independent of the state number, i.e., around 85% of Ne_2^+ and 15% of Ne_3^+. Finally, when dynamics starts on the highest-energy state, dissociation is quite extensive and produces 45% of Ne^+, 55% of Ne_2^+, and no Ne_3^+. This fast and extensive fragmentation can be explained by two factors: the high total initial energy and the repulsive character of these highest-energy states.

This state-dependent fragmentation and the double peak in the time evolution of the nanodroplet size distributions reveal the coexistence of two different types of dynamics: fast and explosive when starting on one of the highest-energy states, and slower therefore leaving more time for the friction to stabilize larger fragments when starting on one of the lowest-energy states.

IV. RESULTS FOR Ne_n, $n=3$–14

A. Final fragment proportions

We now turn to examine the effect of the helium nanodroplet environment on the dissociative ionization of Ne_n, $n=3$–14. For $n\geqslant 5$ the experimental results are not detailed because of the complexity of deconvoluting the fragment distributions as a function of the parent ion size.[49] Therefore no direct comparison is possible. The final proportions of Ne^+, Ne_2^+, Ne_3^+, and Ne_4^+ fragments are presented in Fig. 6 as a function of the initial cluster size for three different cases: results obtained for free neon clusters, for neon clusters embedded in an infinite-size helium droplet, and for neon clusters in a 1100-atom nanodroplet. As discussed in the previous section, the helium environment is modeled by a friction coefficient of 2.5 a.u. The free cluster results have

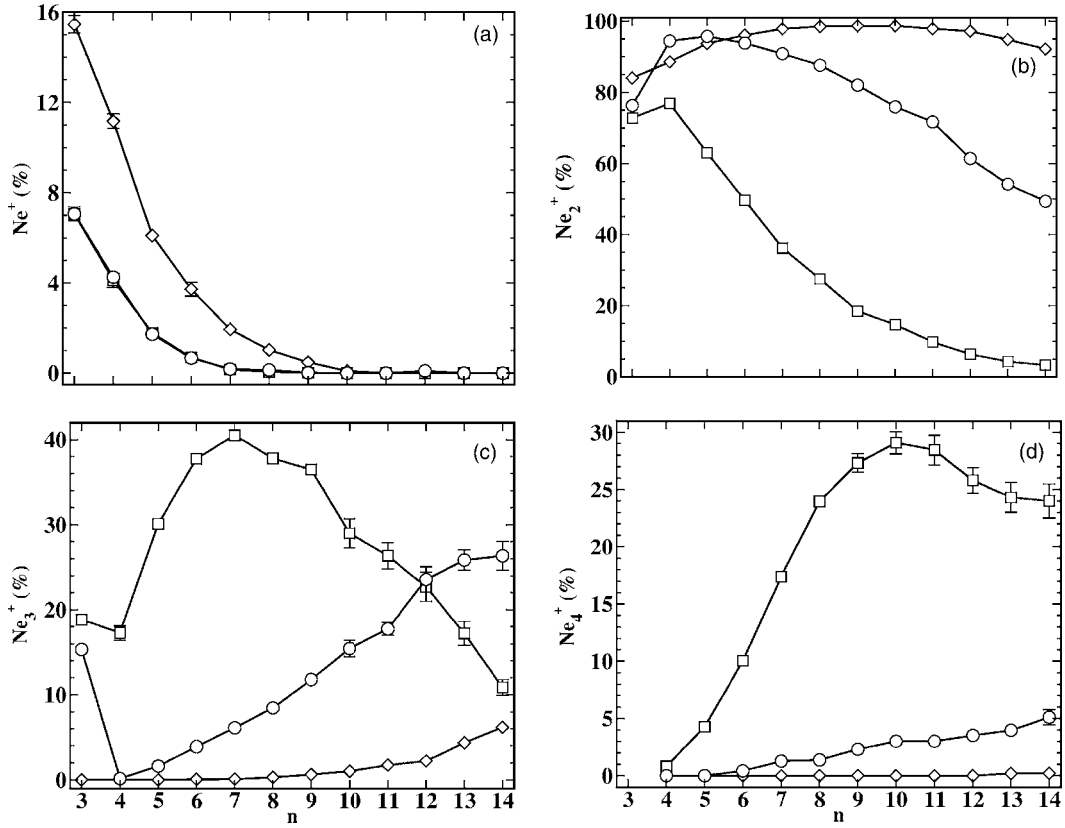

FIG. 6. Final proportions of (a) Ne^+, (b) Ne_2^+, (c) Ne_3^+, and (d) Ne_4^+ fragments as a function of the initial cluster size for the fragmentation of free $(Ne_n^+)^*$ (diamonds), $(Ne_n^+)^*$ embedded in infinite (squares), and finite $N=1100$ (circles) size helium nanodroplets.

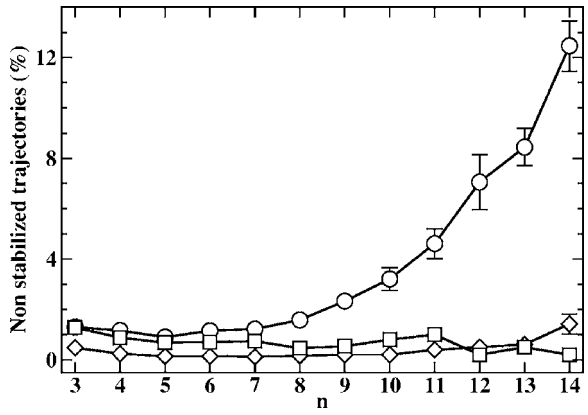

FIG. 7. Final proportion of nonstabilized trajectories for free $(Ne_n^+)^*$ (diamonds) or $(Ne_n^+)^*$ embedded in infinite (squares) or finite $N=1100$ (circles) size helium nanodroplets.

been presented in our previous publication[32] and are reported here for ease of comparison. Briefly, free cluster ionization leads to extensive fragmentation, Ne_2^+ being the main fragment for all studied sizes with a maximum of 99% for $n=8-10$. The next important fragment is Ne^+ for $n<9$ and Ne_3^+ for $n>9$. No Ne_4^+ is detected, except in very small proportion for $n=13$–14.

In the infinite-size helium droplets the effect of friction, as expected, is to stabilize larger fragments, but fragmentation is not completely caged. Ne_2^+ is still the main fragment for $n\leqslant 6$, then larger fragments become more and more abundant: Ne_3^+ for $6<n\leqslant 10$, then Ne_4^+, … . The accident in the Ne_2^+ and Ne_3^+ fragment proportions for $n=3$ is due to the very weak coupling between the A' and A'' classes of planar symmetry, which leads to stable Ne_3^+ clusters in the A'' excited states.[50]

For the finite-size helium nanodroplet, the effect of the friction is similar to the infinite-size one but to a lower extent. Ne_2^+ is the main fragment for all the studied sizes, but its proportion is down to about 50% for $n=14$, while the proportion of Ne_3^+ is steadily growing up to 26% for $n=4$–14. The proportion of Ne_4^+ becomes non-negligible for $n\geqslant 6$ and slowly increases up to 5% for $n=14$. One remarkable feature is that the dependence of the proportion of Ne^+ as a function of the parent ion size is the same one in both the infinite- and the finite-size helium droplets. This is due to the fact that Ne^+ comes from the highest, repulsive energy states for which dissociation is very fast and energetic. By the time dynamics is over, only a limited amount of energy has been transferred to the helium environment by friction, so that even the smallest 1100-atom droplet has not been evaporated and the effect of friction is similar to the infinite-size helium droplet case.

B. Long-lived excited species

The case of the parent ion sizes $n\geqslant 9$ in a finite-size nanodroplet deserves special attention. The dynamics of these clusters leads to a non-negligible number of trajectories for which fragments are not stabilized after 100 ps propagation, as shown in Fig. 7. For $\gamma=2.5$ a.u. and $N=1100$, the number of unfinished trajectories exhibits a sharp increase at $n\geqslant 9$ and reaches about 12.5% for $n=14$, whereas for $\gamma=0$ a.u. and for $\gamma=2.5$ a.u. in the infinite nanodroplet case, no more than 1.4% of the trajectories reach the time limit. These unfinished trajectories correspond to Ne_p^+ species that are still evolving, i.e., not fragmenting but not declared stable by the stabilization criterion used (a Ne_p^+ fragment is considered as stable if its internal energy is smaller than the classical minimum of Ne_{p-1}^+). For instance, out of the 12.5% of unfinished trajectories for $n=14$, 1.5% correspond to Ne_3^+, 3.7% to Ne_4^+, and the remaining 7.3% to Ne_p^+ with $5\leqslant p\leqslant 10$. We have checked that the kinetic energy in these trajectories is not small, which excludes the case of Ne_p^+ trapped in a local potential well with atomic velocities below the Landau critical velocity. The total energy of these long-lived species is constant, which means that the helium droplet environment is completely evaporated, or the remaining cluster has ejected itself from the droplet. These trajectories are therefore trapped in an excited potential well with very weak coupling to other electronic states, or in a well of the ground potential-energy surface behind a barrier preventing dissociation. In the case of the infinite-size helium droplet, these systems would keep losing energy by friction until reaching stabilization.

C. Dependence on the ionization mechanism

Initial conditions used in this work were designed to reproduce very rapid ionization by an $\simeq$60 eV electron. In this case the ionization process is equivalent to coherent ionization by a wide energy light pulse ("white light") and all the initial states of the ion are coherently excited. This is modeled by using as initial conditions a wave packet with equal coefficients on all the electronic states and by starting the classical dynamics equiprobably on any of the surfaces. However, ionization inside a helium nanodroplet[51,52] proceeds in a different way. Because there are so many more helium atoms than neon atoms, the incoming electron first ionizes a helium atom. This initial step is followed by a series of charge hops,[19,22,53] until the electronic hole reaches the vicinity of the neon cluster. The neon cluster is then ionized by charge transfer from He^+ to Ne_n, which is a state-to-state process. This can be modeled by starting the initial wave packet on one electronic state only. We have checked on the case of Ne_4 and Ne_9 in an infinite-size droplet that the dissociation results are not significantly affected by this change of initial conditions. However, we have seen that the fragmentation is strongly affected by the initial electronic state on which the dynamics starts. Hence if the charge transfer favors some of the electronic states the results can be different. A specific study of the charge-transfer mechanism would be required in order to answer this question.

V. DISCUSSION AND CONCLUSIONS

We have studied the effect of the helium nanodroplet environment on the fragmentation of neon clusters upon ionization, for clusters with 3–14 atoms, taking into account all the potential-energy surfaces involved and their couplings, and modeling the influence of the helium environment by a

friction force. By comparison with existing experimental results we have set a reasonable estimation for the corresponding friction coefficient, $\gamma=2.5$ a.u.

As expected, the main effect of the friction is shown to stabilize larger fragments. This effect is very important for very large nanodroplets, but not enough to completely "cage" the dissociation. For smaller size helium droplets the effect is less important. Ne_2^+ is the main fragment as in the case of free neon clusters, although its proportion is strongly decreased (50% instead of 92% for $n=14$). One surprising result is the existence of long-lived trajectories for small helium nanodroplets. The droplet is completely evaporated and the neon clusters are trapped in a local potential well with non-negligible kinetic energy. This is similar to the stabilization in helium droplets of nonthermodynamically stable species such as the triplet state of alkali dimers[6,54] or isomers of van der Waals molecules that are not encountered in the gas phase.[7,55–57]

The value we have obtained for the friction coefficient, $\gamma=2.5$ a.u., is rather large compared to the value for Na^+ in bulk helium, 0.078 a.u.[34] This may imply that some of the assumptions in our phenomenological model are not fulfilled and/or that the friction coefficient includes other effects that are not explicitly taken into account. One of the assumptions we have made is that evaporating helium atoms remove their average binding energy from the system. If they were ejected with nonzero kinetic energy, then fewer helium atoms would be required to dissipate the same amount of energy. Recently, Lewis *et al.*[25] have shown that the first 5000 helium atoms can remove roughly 22 cm^{-1}/at., which is five to six times the mean binding energy in the droplets we have studied. With this value, the results we have obtained for a 3300-atom nanodroplet could actually correspond to a much smaller atom nanodroplet. This would mean that a smaller friction coefficient could be used for the experimental sizes in order to reproduce the results of Ruchti *et al.* in Fig. 1. However, the kinetics of the parent ion fragmentation sets limits on the possible values for the friction coefficient. If any effect is to be observed, the velocity relaxation time (i.e., the time constant of the exponentially decreasing velocity of a neon atom in the absence of any potential) has to be shorter than or at least of the same order of magnitude as the parent ion lifetime. The velocity relaxation times corresponding to $\gamma=0.078$, 0.75, 2.5, and 7.5 a.u. are 11.3, 1.2, 0.35, and 0.12 ps, respectively. The parent ion lifetimes of free Ne_n^+ clusters spread from 0.3 to 0.8 ps.[32] For $(Ne_4^+)^*$ it is about 0.4 ps when spin-orbit interaction is included. Hence for $\gamma \leqslant 0.75$ a.u. the friction does not have enough time to cage the Ne_3^+ fragment, whereas for $\gamma=7.5$ a.u. the effect of the friction is close to its maximum since the velocity relaxation time is then about three times shorter than the parent ion lifetime: increasing the friction coefficient above this value should not bring any significant changes in the final fragment proportions. A friction coefficient close to the value for Na^+ in bulk helium, 0.078 a.u., will then show no effect from friction on the fragmentation pattern. Increasing the energy removed by the evaporating helium atoms would bring the calculated results closer to the infinite droplet limit, but even in infinite droplets $\gamma=0.75$ a.u. is the smallest value for which a friction effect can be seen.

The simplicity of the model used here has the advantage that only one parameter, the friction coefficient, was fitted. The counterpart of this simplicity is the possible inclusion, through the friction coefficient, of other effects that are not explicitly taken into account. One of them is the formation of a "snowball" around the charged neons, characterized by a solidlike structure. Atkins[58] estimated that around 50 helium atoms were dragged by ions during their motion in bulk helium. Experimental mobility measurements on the alkali ions by Glaberson and Johnson[59] have shown that the number of helium atoms depends on the identity of the core ion. Variational Monte Carlo calculations[60] on the Li^+, Na^+, K^+, and Cs^+ alkali ions found that the numbers of helium atoms attached to the core ion were 3, 12, 17, and 2, respectively. Concerning neon ions, the existence of a snowball with solidlike structure is unlikely. Mass spectrometry experiments by Ruchti *et al.*[23] and by Brindle *et al.*[61] have indeed shown that there is no "magic number." These experimental results were confirmed by diffusion Monte Carlo calculations[61] that could not find any extra stability for any number of helium atoms attached to Ne^+, between 3 and 14. Only the first two atoms that build the ionic $(NeHe_2)^+$ core are rigidly attached to Ne^+. Ion drift experiments,[35] on the other hand, suggest that Ne^+He_n has a magic number for $n=11$. In addition, the time constant for the formation of these snowballs is unknown. It would also be important to know the other processes taking place inside helium nanodroplets (individual collisions with the helium atoms as suggested by Braun and Drabbels' experiment[26,62] for high-energy photodissociation of CH_3I, collective quantum dynamics of the helium as advocated by Takayanagi and Shiga,[27] …). This will be the focus of a future publication in which the motion of the helium atoms will be explicitly taken into account.

It would be very interesting to compare the behavior of neon clusters to the one of other rare gases. By changing the nature of the rare gas (Rg), the mass, the internal energy available for dissociation, and the magnitude of the spin-orbit interaction are changed. A heavier mass gives a smaller effect of the friction for a given value of the friction coefficient. The amount of energy available for dissociation is directly related to the Rg_2^+ well depth since vertical ionization produces the cluster ion in the region of asymptotic distances, and larger available energies lead to more extensive dissociation. Finally, a stronger spin-orbit interaction affects both the initial conditions and the couplings during the dynamics. It affects the initial conditions because of the splitting of the potential-energy curves in the region reached by vertical ionization in two groups of states going asymptotically to $Rg^+(^2P_{3/2})+(n-1)Rg$ and $Rg^+(^2P_{1/2})+(n-1)Rg$. It also increases the coupling between electronic states which can induce more transitions and accelerate the relaxation and fragmentation. It is therefore interesting to study the dynamics of Rg_n^+ both in vacuum and inside helium droplets.

ACKNOWLEDGMENTS

The authors would like to thank Marius Lewerenz and Ken Janda for fruitful discussions and strong interest in this work. The authors express all their gratitude to Manuel Barranco for lending his DFT code. The Calmip computer center of Toulouse is gratefully acknowledged for a grant of computer time. One of the authors (D.B.) thanks the Paul Sabatier University of Toulouse for financial support through an ATUPS grant.

[1] P. Sindzingre, M. L. Klein, and D. M. Ceperley, Phys. Rev. Lett. **63**, 1601 (1989).
[2] S. Grebenev, J. P. Toennies, and A. F. Vilesov, Science **279**, 2083 (1998).
[3] M. Hartmann, R. E. Miller, J. P. Toennies, and A. Vilesov, Phys. Rev. Lett. **75**, 1566 (1995).
[4] J. P. Toennies and A. F. Vilesov, Annu. Rev. Phys. Chem. **49**, 1 (1998).
[5] K. K. Lehmann and G. Scoles, Science **279**, 2065 (1998).
[6] J. P. Higgins, J. Reho, F. Stienkemeier, W. E. Ernst, K. K. Lehmann, and G. Scoles, in *Atomic and Molecular Beams: The State of the Art 2000*, edited by R. Campargue (Springer, Berlin, 2000), pp. 723–754.
[7] K. Nauta and R. E. Miller, in *Atomic and Molecular Beams: The State of the Art 2000*, edited by R. Campargue (Springer, Berlin, 2000), pp. 775–792.
[8] E. Lugovoj, J. P. Toennies, and A. Vilesov, J. Chem. Phys. **112**, 8217 (2000).
[9] K. Callegari, K. K. Lehmann, R. Schmied, and G. Scoles, J. Chem. Phys. **115**, 10090 (2001).
[10] J. P. Toennies and A. F. Vilesov, Angew. Chem. **43**, 2622 (2004).
[11] J. Chem. Phys. **115** (2001), special issue on Helium Nanodroplets: A Novel Medium for Chemistry and Physics.
[12] M. Hartmann, F. Mielke, J. P. Toennies, A. Vilesov, and G. Benedek, Phys. Rev. Lett. **76**, 4560 (1996).
[13] K. Nauta and R. E. Miller, J. Phys. C **115**, 8384 (2001).
[14] R. E. Zillich and K. B. Whaley, Phys. Rev. B **69**, 104517 (2004).
[15] R. E. Zillich, Y. Kwon, and K. B. Whaley, Phys. Rev. Lett. **93**, 250401 (2004).
[16] M. Hartmann, A. Lindinger, J. P. Toennies, and A. F. Vilesov, Phys. Chem. Chem. Phys. **4**, 4839 (2002).
[17] R. Lehnig and A. Slenczka, J. Chem. Phys. **122**, 244317 (2005).
[18] H. Hoshina, J. Lucrezi, M. N. Slipchenko, K. E. Kuyanov, and A. F. Vilesov, Phys. Rev. Lett. **94**, 195301 (2005).
[19] A. Scheidemann, B. Schilling, and J. P. Toennies, J. Phys. C **97**, 2128 (1993).
[20] R. Frochtenicht, U. Henne, J. P. Toennies, A. Ding, M. Fieber-Erdmann, and T. Drewello, J. Chem. Phys. **104**, 2548 (1995).
[21] B. E. Callicoatt, D. D. Mar, V. A. Apkarian, and K. C. Janda, J. Chem. Phys. **105**, 7872 (1996).
[22] B. E. Callicoatt, K. Förde, T. Ruchti, L. Jung, K. C. Janda, and N. Halberstadt, J. Chem. Phys. **108**, 9371 (1998).
[23] T. Ruchti, K. Förde, B. E. Callicoatt, H. Ludwigs, and K. C. Janda, J. Chem. Phys. **109**, 10679 (1998).
[24] T. Ruchti, B. E. Callicoat, and K. C. Janda, Phys. Chem. Chem. Phys. **2**, 4075 (2000).
[25] W. K. Lewis, B. E. Applegate, J. Sztáray, B. Sztáray, T. Baer, R. J. Bernish, and R. E. Miller, J. Am. Chem. Soc. **126**, 11283 (2004).
[26] A. Braun and M. Drabbels, Phys. Rev. Lett. **93**, 253401 (2004).
[27] T. Takayanagi and M. Shiga, Chem. Phys. Lett. **372**, 90 (2003).
[28] H. Haberland, Surf. Sci. **156**, 305 (1985).
[29] U. Buck and H. Meyer, J. Chem. Phys. **84**, 4854 (1986).
[30] U. Buck, J. Phys. Chem. **92**, 1023 (1988).
[31] P. Lohbrandt, R. Galonska, H. Kim, M. Schmidt, C. Lauenstein, and U. Buck, in *Atomic and Molecular Beams: The State of the Art 2000*, edited by R. Campargue (Springer, Berlin, 2000), pp. 623–636.
[32] D. Bonhommeau, A. Viel, and N. Halberstadt, J. Chem. Phys. **123**, 54316 (2005).
[33] D. Bonhommeau, A. Viel, and N. Halberstadt, J. Chem. Phys. **120**, 11359 (2004).
[34] H. Günther, M. Foerste, G. zu Putlitz, and T. Schumacher, Low Temp. Phys. **22**, 143 (1996); Fiz. Nizk. Temp. **22**, 189 (1996).
[35] T. M. Kojima, N. Kobayashi, and Y. Kaneko, Z. Phys. D: At., Mol. Clusters **22**, 645 (1992).
[36] N. Saito, T. M. Kojima, N. Kobayashi, and Y. Kaneko, J. Chem. Phys. **100**, 5726 (1994).
[37] J. C. Tully, J. Chem. Phys. **93**, 1061 (1990).
[38] U. Müller and G. Stock, J. Chem. Phys. **107**, 6230 (1997).
[39] D. R. Allum, P. V. E. McClintock, A. Phillips, and R. M. Bowley, Phil. Trans. Roy. Soc. **284**, 23 (1977).
[40] M. Lewerenz, B. Schilling, and J. P. Toennies, J. Chem. Phys. **102**, 8191 (1995).
[41] M. Barranco and E. S. Hernández, Phys. Rev. B **49**, 12078 (1994).
[42] S. M. Gatica, E. S. Hernández, and M. Barranco, J. Chem. Phys. **107**, 927 (1997).
[43] M. Barranco, E. S. Hernández, R. Mayol, and M. Pi, Phys. Rev. B **69**, 134502 (2004).
[44] R. De Bruyn Ouboter and C. N. Yang, Physica B & C **44**, 127 (1987).
[45] J. Boronat, J. Casulleras, and J. Navarro, Phys. Rev. B **50**, 3427 (1994).
[46] F. Dalfovo, A. Lastri, L. Pricaupenko, S. Stringari, and J. Treiner, Phys. Rev. B **52**, 1193 (1995).
[47] K. C. Janda (private communication).
[48] The droplet size for which this sharp increase in the proportion of Ne_4^+ occurs is subject to some corrections: on the one hand the droplets may have been larger than the published sizes according to experimentalists, and on the other hand about 500 atoms are evaporated in the pickup process. In any case the experimental sizes are given as indicative sizes which are averaged over a size distribution.
[49] B. Callicoatt, Ph.D. thesis, University of California, 1998.
[50] The A' and A'' classes can in principle be coupled in the presence of friction: these symmetry classes are coupled if the rotational angular momentum of the neon cluster is not zero, which is the case since friction leads to the nonconservation of the rotational angular momentum of the neon cluster.
[51] J. A. Northby, J. Chem. Phys. **115**, 10065 (2001).
[52] J. P. Toennies, in *Proceedings of the 107 Course of the International School of Physics, Enrico Fermi on the Chemical Physics of Atomic and Molecular Clusters* (North-Holland, Amsterdam, 1990), p. 597.
[53] K. R. Atkins, in *Proceedings of the International School of Physics Enrico Fermi, Course XXI on Liquid Helium*, edited by G. Carerei (Academic, New York, 1963), p. 403.
[54] J. P. Higgins, C. Callegari, J. Reho, F. Stienkemeier, W. E. Ernst, M. Gutowski, and G. Scoles, J. Phys. Chem. A **102**, 4952 (1998).
[55] K. Nauta and R. E. Miller, J. Chem. Phys. **111**, 3426 (1999).
[56] K. Nauta and R. E. Miller, Science **287**, 293 (2000).
[57] F. Madeja, M. Havenith, K. Nauta, R. E. Miller, J. Chocholouşová, and P. Hobza, J. Chem. Phys. **120**, 10554 (2004).
[58] K. R. Atkins, Phys. Rev. **116**, 1339 (1959).
[59] W. I. Glaberson and W. W. Johnson, J. Low Temp. Phys. **20**, 313 (1975).
[60] M. Buzzacchi, D. E. Galli, and L. Reatto, Phys. Rev. B **64**, 094512 (2001).
[61] C. A. Brindle, M. R. Prado, K. C. Janda, N. Halberstadt, and M. Lewerenz, J. Chem. Phys. **123**, 064312 (2005).
[62] A. Braun, Ph.D. thesis, École Polytechnique Fédérale de Lausanne, 2004.